JRACR

Journal of Risk Analysis and Crisis Response, 2024, 14(1), 80-90
https://jracr.com/
ISSN Print: 2210-8491
ISSN Online: 2210-8505

Article

Characteristic Analysis of the *M*s6.8 Luding Earthquake Sequence in Sichuan, China, on Sept. 5, 2022

Min Zhao [1,2], Feng Long [1,2,*], Yue Gong [1] and Fang Du [1]

[1] Sichuan Earthquake Agency, Chengdu (610041), Sichuan, China
[2] State Key Laboratory of Geodesy and Earth's Dynamics, Innovation Academy for Precision Measurement Science and Technology, CAS, Wuhan (430077), Hubei, China
* Correspondence: icy1111@163.com

Received: April 28, 2023; Received in revised form: September 12, 2023; Accepted: January 8, 2024; Available online: March 31, 2024

Abstract: The *M*s6.8 earthquake occurred in Luding County, Ganzi Prefecture, Sichuan Province, China at 12:52 p.m. on Sept. 5, 2022, is preliminarily analyzed in terms of regional tectonics, historical earthquakes, sequence characteristics and focal mechanism solutions. The results show that: 1) The magnitude difference ΔM between the main shock and the maximum aftershock, the energy ratio ER of the main shock to the aftershocks, the *p*-value and the estimated M_{max}-value indicate that the *M*s6.8 Luding earthquake sequence can be divided into the main shock-aftershock type (MAT). 2) The spatial distribution of the aftershocks, their corresponding *b*-value and expected maximum magnitude are obviously segmented, which reflect the complexity of the seismogenic tectonics. 3) According to the focal mechanisms obtained from the HASH program, the geometry distribution of the sequence, and the relationship between the sequence and the nearby faults, it can be inferred that the Moxi fault segment of the Xianshuihe fault zone is the seismogenic tectonics of the *M*s6.8 Luding earthquake sequence.

Keywords: The *M*s6.8 Luding Earthquake; Sequence Analysis; The Focal Mechanisms; Seismogenic Tectonics

1. Introduction

At 12:52 on September 5, 2022, local time, a *M*s6.8 earthquake occurred in Luding County, Ganzi Prefecture, Sichuan Province, China. The epicenter is in the Hailuogou Glacier Forest Park, Minya Konka Mountain, only 39 km away from the Luding County and 47 km away from the Kangding City, where Ganzi Prefecture government is located. According to the earthquake intensity map released by the Ministry of Emergency Management (https://www.mem.gov.cn/xw/yjglbgzdt/202209/t20220911_422190.shtml), the maximum intensity of the event is Ⅸ degree. The earthquake has caused serious geological disasters, resulting in the damage to many buildings and infrastructure, causing serious casualties and property losses. As of Sept. 13, 2022, the earthquake and secondary geological disasters caused 93 deaths and 25 losses of communication. The disaster caused by the earthquake has caused widespread concern from all walks of life.

The *M*s6.8 Luding earthquake occurred in the southeast segment of the Xianshuihe fault zone with complex geological tectonics (Figure 1). After the earthquake, international and domestic

seismologists also paid attention to the future strong earthquake risk of the Xianshuihe fault zone. Therefore, the regional tectonic background, historical earthquakes, sequence characteristics and focal mechanism solution of the *Ms*6.8 Luding earthquake are preliminarily analyzed in this paper. It is expected to provide a reference basis for the subsequent study and the seismic risk of the Xianshuihe fault zone.

2. Geological Settings and Historical Earthquakes

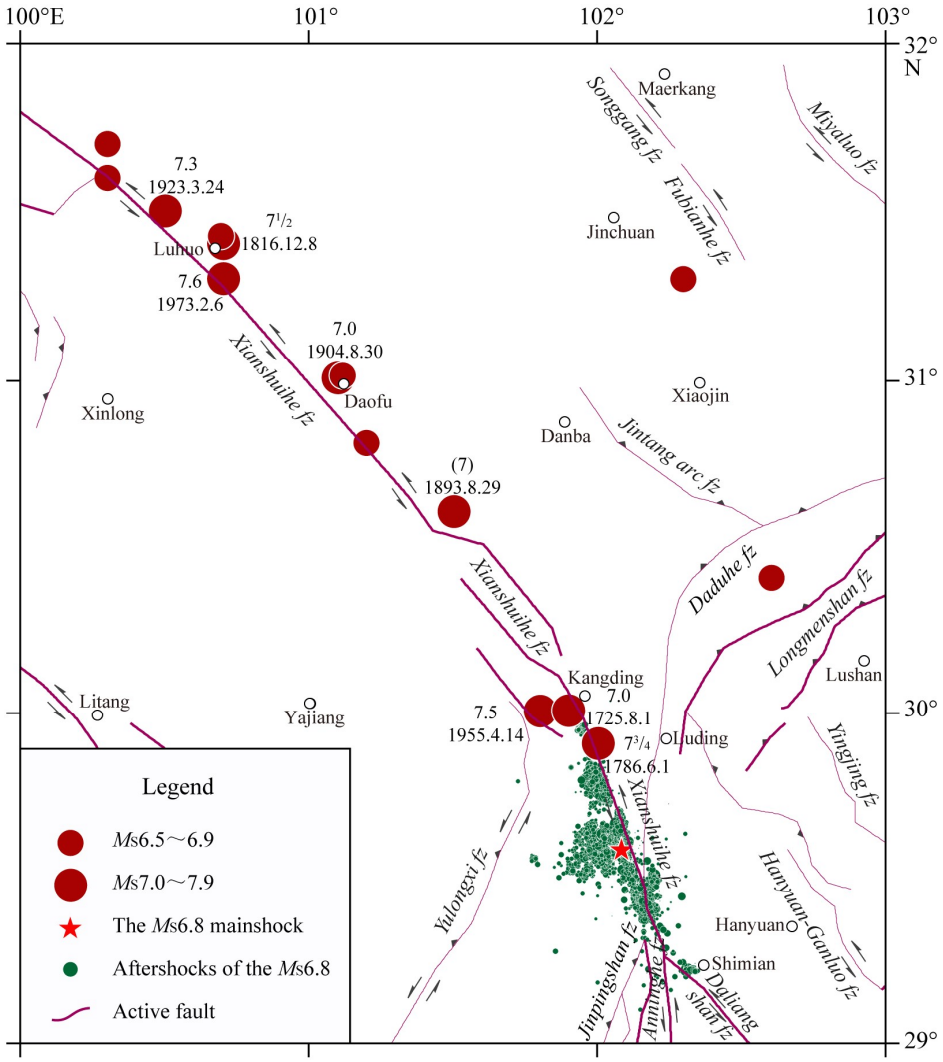

Figure 1. Geological tectonics and historical earthquake distribution along the Xianshuihe fault zone and its vicinity.

The *Ms*6.8 Luding earthquake occurred in the southeast segment of the Xianshuihe fault zone. The Xianshuihe fault zone is in the eastern margin of the Qinghai Tibet Plateau and the middle section of the north-south seismic belt. It is a large left-lateral strike-slip fault in the Songpan Ganzi orogenic belt, with strong Holocene activity. The fault has a total length of more than 400 kilometers, with an overall trend of N40°-50°W. It starts from the northwest of Ganzi in the northwest segment, passes Luhuo, Daofu, Kangding, and Moxi town in Luding in the southeast segment, and gradually weakens to the south of Xinmin town in Shimian, and finally disappears near the Gongyi Sea in Shimian [1-4]. The existing research results show that the activities of the Xianshuihe fault zone since the Holocene can be

divided into two segments with Huiyuansi pull apart basin as the boundary. The northwest segment is about 200 km long and consists of a single main fault, mainly left- lateral strike-slip [5-7]. The southeast segment has complex tectonics, mainly consisting of the Moxi fault segment in NNW direction and the fault segment composed of the Yarra River, Seraha and Zheduotang three branch fault, with a length of about 110 km. The M_S6.8 Luding earthquake located near the Moxi fault segment of the Xianshuihe fault zone with complex tectonics (Figure 1). The Moxi segment of the Xianshuihe fault zone starts from the north and extends to the southeast, passing Moxi, Ertaizi, Wandong, Menghugang, Tianwan and Xinmin, and then extends to Anshun. Later, the new activity of the fault is weakened. The strike is between N20°~40°W, dip SW or NE, and dip angle is N60°~80° [8-9].

The Xianshuihe fault zone is one of the fault zones with the most frequent strong earthquakes and large earthquakes in mainland China [10]. Since historical records, 13 earthquakes with $M_S \geq 6.5$ have occurred along the Xianshuihe fault zone since 1725, including 6 events with M_S6.5-6.9 and 7 events with M_S7.0-7.9. Among them, the largest historical earthquake was the $M_S7^3/_4$ Kangding earthquake in 1786 located in the southeast segment. The M_S6.8 Luding main event is just located about 35 km to the southeast of the $M_S7^3/_4$ Kangding earthquake in 1786. The aftershocks extended to the southeast segment of the rupture zone of the $M_S7^3/_4$ Kangding earthquake in 1786 [10-11].

3. Overview of Sequences

According to the Sichuan Seismic Network (SSN), about 4023 aftershocks with $M_L \geq 0.0$ have been recorded by Sept. 20, 2022, including 63 aftershocks of M_L3.0-3.9, 3 aftershocks of M_L4.0-4.9 and 1 aftershock of M_L5.0-5.9, that is, the maximum aftershock of M_S4.5(M_L5.1) occurred on Sept. 7,2022. The $M_L \geq 4.0$ aftershocks are listed in Table 1.

Table 1. The $M_L \geq 4.0$ aftershocks of the M_S6.8 Luding earthquake sequence.

Serial No.	Time of the event		Location		Magnitude	Focal depth
	Y-M-D	H:M:S	Longitude λ/°E	Latitude φ/°N	M_L	km
1	2022-09-05	12:52:18	102.08	29.59	M_S6.8	16
2	2022-09-05	12:56:34	102.18	29.40	4.5	15
3	2022-09-05	17:39:21	102.17	29.38	4.0	18
4	2022-09-05	19:26:20	102.18	29.48	4.2	17
5	2022-09-07	02:42:15	102.15	29.42	5.1/M_S4.5	17

The time-sequence of *M-T*, *N-T* and Δ *T-T* diagrams (Figure 2) show that the $M_L \geq 0.0$ aftershocks are abundant after the mainshock, but the intensity of the aftershocks are not high. In order to reveal the sequence characteristics quantitatively, the magnitude completeness (M_c) is determined by the Goodness-of-fit test (GFT) [12] method as to M_L1.7 (Figure 3a), and then the *b*- and *p*-values, which demonstrate the stress state and temporal decay of the sequence, respectively, determined by fitting the G-R relationship [13] and the revised Omori's law [14-15].The results derived from the first 24 hours catalog of magnitude greater than the M_c show that the *b*-value is 0.696 (Figure 3a).This result reflects the strong stress disturbance at the early stage of the aftershock sequence. The calculated *p*-value is 1.24 (Figure 3b). It indicates that the early sequence attenuates

rapidly after the main earthquake. The M_{max}-value, defined by a/b, is estimated to M_L5.2 (M_S4.5), which is very close to the actual biggest aftershock, the M_L5.1 Shimian event at 02:42, Sept. 7,2022 local time. It indicates that the maximum aftershock with high probability may have occurred, and the event in the sequence is not foreshock.

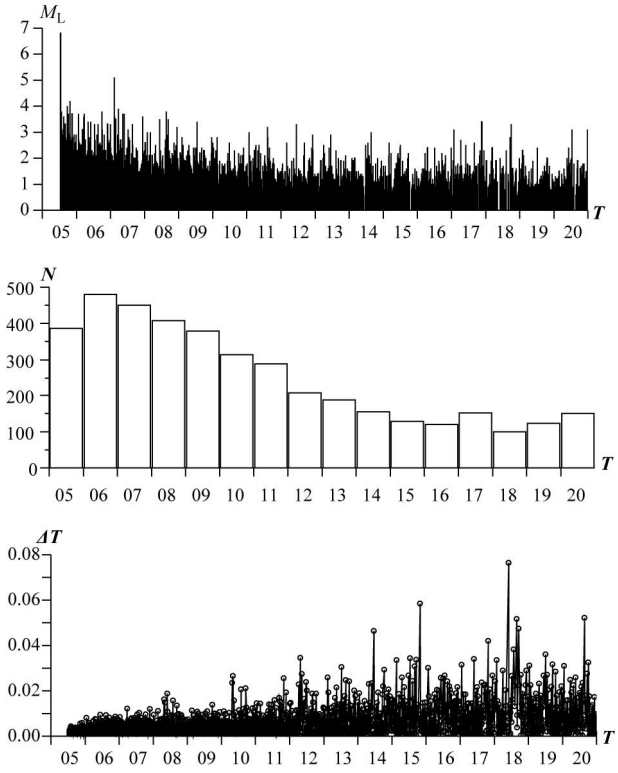

Figure 2. The time-sequence diagrams of *M-T*, *N-T* and ⊿*T-T*.

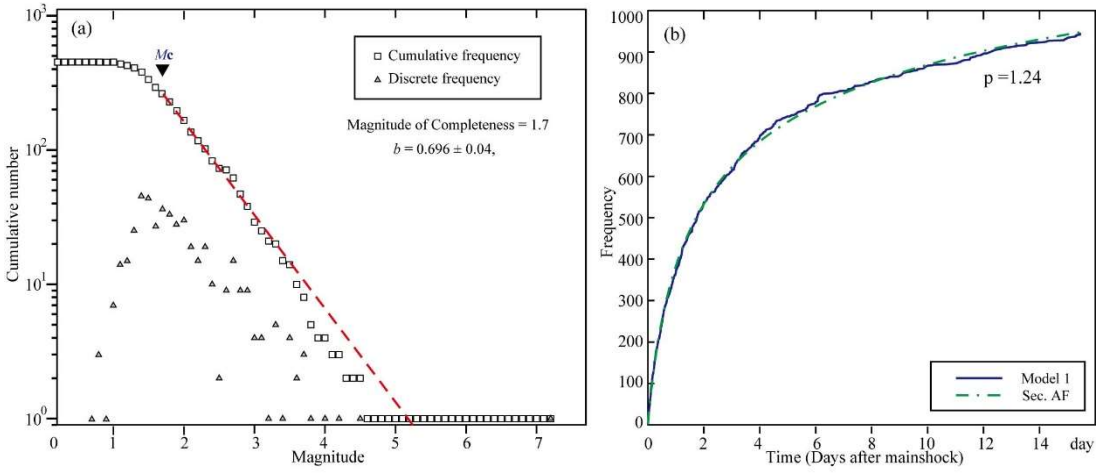

(a) The G-R relationship fit. **(b)** The revised Omori's law fit.

Figure 3. Two fitting curves of the M_S6.8 Luding earthquake sequence.

Two methods are used to evaluate the type of earthquake sequence: one is the magnitude difference Δ*M*, denoted as the magnitude difference between the mainshock and the maximum aftershock [16], and other is the energy ratio E_R, defined as the elastic energy ratio of the mainshock

to the whole sequence [17]. Generally, the elastic energy is estimated from the magnitude according to the formula [18].

$$\log E = 1.44 M_S + 12.52$$

The ΔM=2.3 and E_R=99.97% indicate that the *M*s6.8 Luding earthquake sequence is a Mainshock-Aftershock Type (MAT). It can be inferred that there will be no aftershocks larger than the main shock magnitude in the sequence, which is consistent with the estimate of the M_{max}-value.

4. Spatial Evolution of Aftershocks

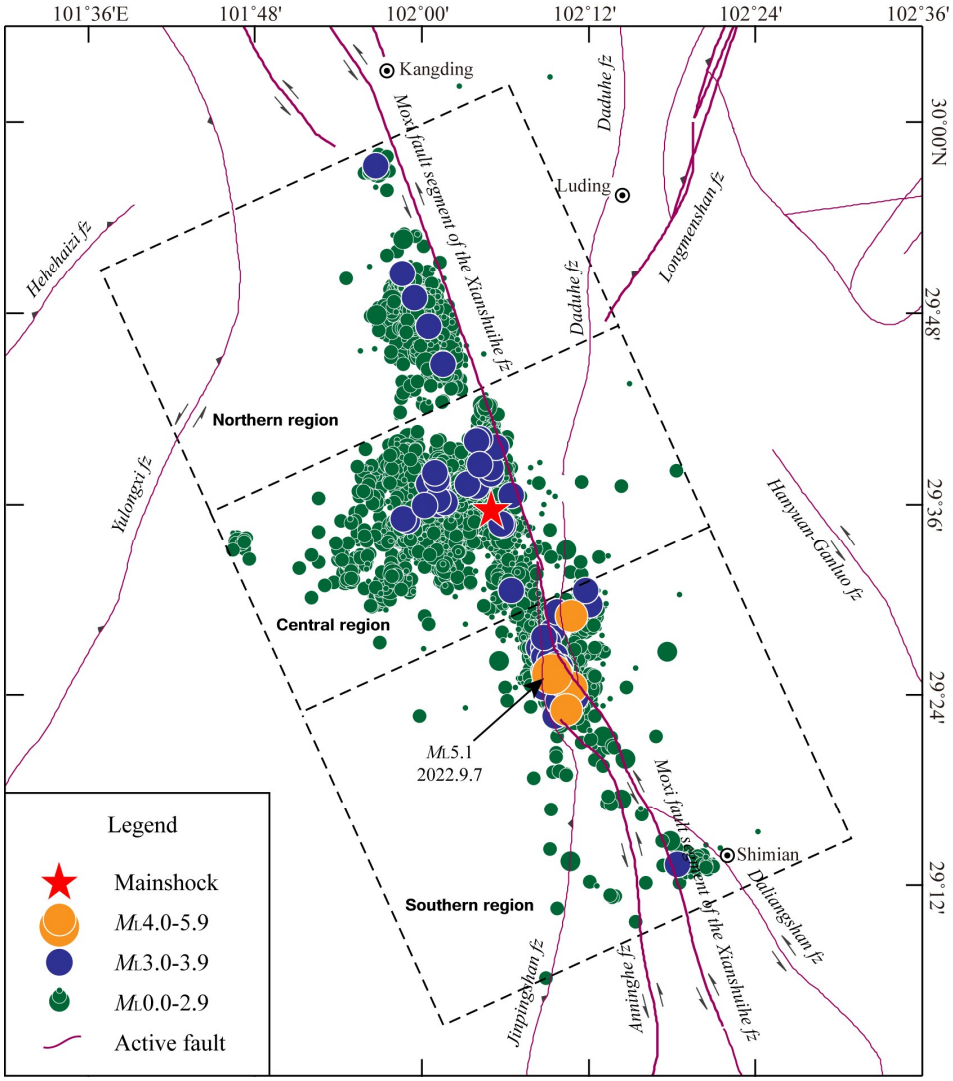

Figure 4. Epicentral map of the *M*s6.8 Luding earthquake sequence.

The epicentral map of the Luding earthquake sequence shows that the aftershocks are distributed along the south-east branch rupture of the Moxi fault segment of the Xianshuihe fault zone, with an overall NW trend and a dense aftershock area of about 65 km in the long axis and about 25 km in the short axis. The aftershock distribution along the fault is divided into three areas (dotted line in Figure 4). The aftershocks in the northern region show relatively low frequency and magnitude activities, strike NW-SE direction, and are consistent with the Moxi fault segment. The length of its major axis and minor axis are about 18 km and 8 km respectively. The aftershocks in the southern region have the same distribution trend, while the frequency and magnitude in the aftershock

sequence in the south region are significantly stronger than those in the northern region. The M_L4.0 aftershocks in the sequence, including the largest aftershock, all occur in the region. The length of its long and short axes is about 14 km and 8 km respectively. The aftershocks in the central region where the M_S6.8 earthquake is located have the highest seismic activity frequency. The aftershocks are distributed in the NEE and NW directions perpendicular to and along the Moxi fault segment, respectively. Different from the aftershocks in other two regions, the two axes of aftershocks distribution are about 23 km and 12 km separately.

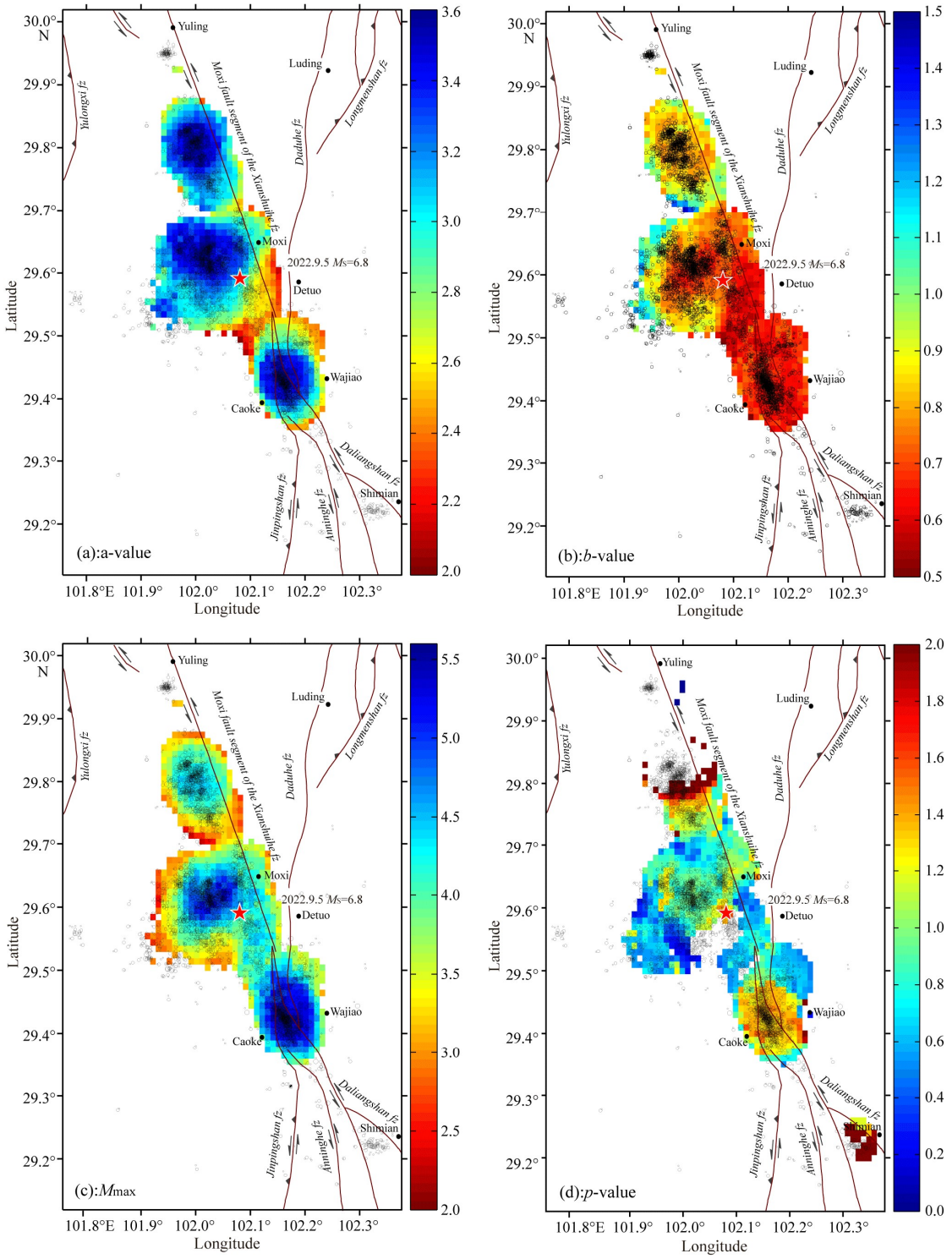

Figure 5. Maps of spatial seismicity parameter.

To study the spatial characteristics of the sequence, the seismicity parameter map of the aftershock area is drawn. The *a*-value diagram (Figure 5a) shows that the aftershock activity rates of the above three subregions are very high, and the cumulative composite frequencies of $M_L \geq 0.0$ events are greater than 3000. The *b*-value diagram (Figure 5b) shows that the south region has the lowest *b*-value, that is, the highest stress field. It is notable that the eastern part of the central region, where the Moxi fault segment is locked, also has a low *b*-value, while the *b*-value in western part is relatively high, which indicating the seismogenic tectonics in the central region are complicated. The M_{max} map (Figure 5c) shows that the maximum expected magnitude in the southern and central regions is relatively high, which may reach M_L5.5, but it may be estimated to be 4.0 in the northern region. The *p*-value map (Figure 5d) demonstrated the seismicity in northern and southern regions decaying faster than that in central region, showing the segmentation difference of the seismogenic tectonics.

The historical earthquake sequences on the same fault are also of reference significance for studying and judging the subsequent earthquake trend, so the historical earthquake sequences on the Xianshuihe fault zone are also compared and analyzed. According to the existing research data, among the earthquakes with the $M_S \geq 6.5$ in the Xianshuihe fault zone, there are only two earthquake cases with clear earthquake types since 1970: the M_S7.6 Luhuo earthquake occurred in 1973 is a mainshock-aftershock type sequence, with its maximum aftershock is a M_S6.3 event (Figure 6a). The sequence is generated by strike-slip faulting and decayed rapidly; the M_S6.9 Daofu earthquake occurred in 1981, with its maximum aftershock M_S3.9 (Figure 6b), which is an isolate-type sequence, also in the strike-slip fault [19-21]. From the only two historical earthquake sequence cases, the earthquake rupture type is consistent with the strike-slip property of the Xianshuihe fault zone, and the sequence types are the mainshock-aftershock type and isolated type respectively. The two historical sequences mentioned above attenuated rapidly, and the largest aftershock occurred within 2 days after the main shock. Therefore, with the two historical sequences as a reference, the M_S6.8 Luding earthquake sequence is unlikely to have subsequent aftershocks of the same intensity as the main shock.

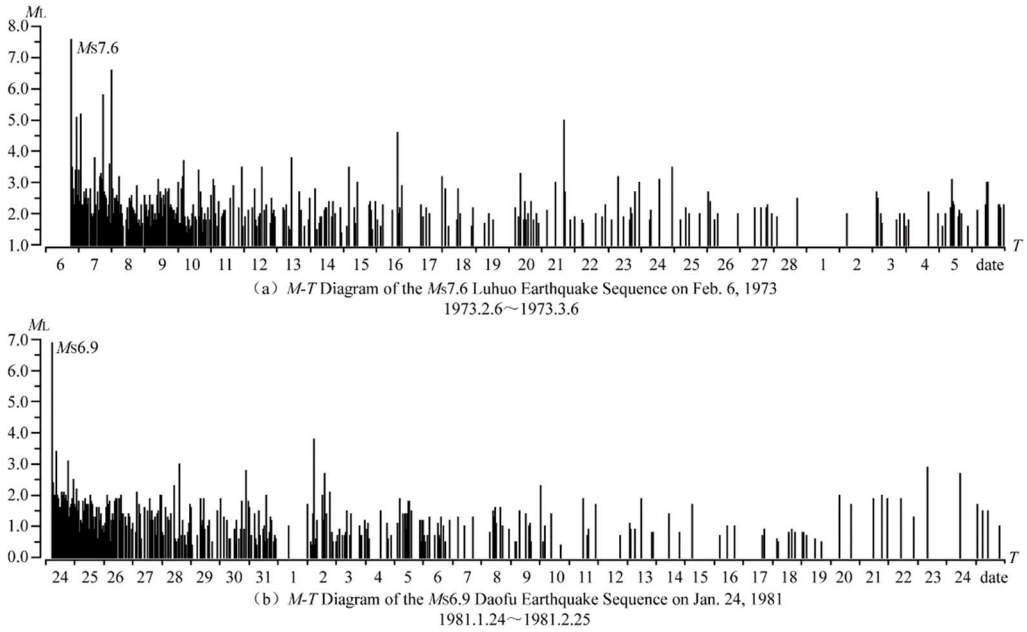

Figure 6. Historical earthquake sequence along the Xianshuihe fault zone.

5. Focal Mechanism Solution

First motion polarities of the *M*s6.8 mainshock and the *M*s4.5 event are picked from a total number of the 38 stations within the epicentral distance of 200 km, and then, the focal mechanisms are calculated by the HASH program [22-23]. The main shock and maximum aftershock have the same focal mechanisms (Figure 7 and Table 2), however, a bit difference in misfit due to a four reading errors caused by the relative lower signal-to-noise of the *M*s4.5 event. Considering the trending direction of the Xianshuihe fault zone and the long-axis of the sequence, the NW-SE striking plane is determined as seismogenic fault plane, that is, the left-lateral strike-slip nodal 2 is the fault plane, which is consistent with the published results [24-27]. The azimuth of P-axis is NWW, which is consistent with the principal compressive direction [28-30], indicating the *M*s6.8 Luding earthquake sequence is controlled by the local geological stress.

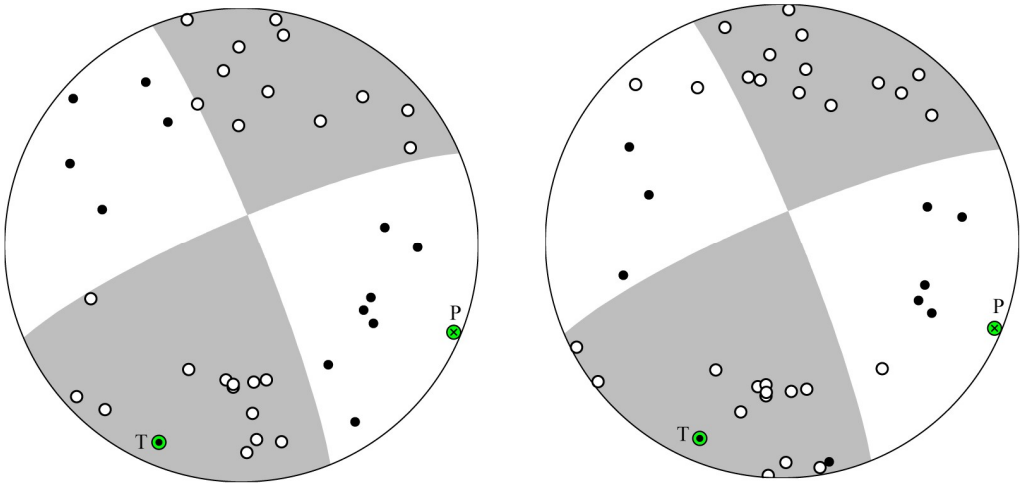

(a) The *M*s6.8 earthquake on Sept. 5, 2022. **(b)** The *M*s4.5 aftershock on Sept. 7, 2022.

Figure 7. Focal mechanism solution of the mainshock and the maximum aftershock.

Table 2. Focal mechanisms for *M*s6.8 and *M*s4.5 events.

Date of the event	Event *M*s	Nodal 1			Nodal 2			P-axis		T-axis		B-axis		Misfit
		strike	dip	rake	strike	dip	rake	az	pl	az	pl	az	pl	
2022-09-05	6.8	247	81	174	338	84	9	112	2	203	11	11	79	0.0
2022-09-07	4.5	247	81	174	338	84	9	112	2	203	11	11	79	0.1

6. Discussion

Xianshuihe fault belt is one of the most active structures in western China, with behaviors in high slip rate (~10mm/a) and frequent reoccurrence period (~100 years). The ruptures of historic strong earthquakes almost cover the whole fault zone length. Although the *M*s6.8 Luding earthquake has released some energy, the southern section of the Xianshuihe fault belt is still at risk of earthquake hazards, that's because (1) the *M*s6.8 Luding earthquake located in the seismic gap generated by the

rupture zone of the M_S7¾ Luding earthquake, 1785 [11], the 64km-length newly ruptured area do not fulfill the historical gap, the rest parts (barriers or asperities) accumulate a lot of energy, (2) the southern segment of the Xianshuihe fault is in the Coulomb static stress increasing regions of the M_S7.0 Lushan earthquake, 2013 [31] and M_S6.3 Kangding earthquake, 2014 [32-33], which showing that the future strong earthquakes in this region is imminent.

7. Conclusions

The M_S6.8 Luding earthquake occurred on the Moxi fault segment of the Xianshuihe fault zone at 12:52 p.m. on Sept. 5, 2022, local time is preliminarily analyzed in terms of regional tectonics, historical earthquakes, sequence characteristics and focal mechanism solutions. The conclusions are summarized as:

1) The magnitude difference ΔM=2.3 between the main shock and the maximum aftershock, the energy ratio E_R≈99.99% of the main shock to the aftershocks, the p-value=1.24 and the estimated M_{max}-value indicate that the M_S6.8 Luding earthquake sequence can be divided into the main shock-aftershock type (MAT).

2) The spatial distribution of the aftershocks, their corresponding b-value and expected maximum magnitude are obviously segmented, which reflect the complexity of the seismogenic tectonics. The sequence behavior in strong segmentation which can be divided into three regions with each seismic characteristic. The southern region of the aftershock distribution is a fast decayed segment with high stress level and seismicity rate. The central region of the aftershock distribution, where the mainshock located at, showed an inhomogeneous b-value distribution, indicating the complexity of the seismogenic tectonics. The northern region of the aftershock distribution has the lowest stress level and expectation maximum magnitude.

3) According to the focal mechanisms obtained from the HASH program, the geometry distribution of the sequence, and the relationship between the sequence and the nearby faults, it can be inferred that the Moxi fault segment of the Xianshuihe fault zone is the seismogenic tectonics of the M_S6.8 Luding earthquake sequence. Take the trending directions of the Xianshuihe fault zone and the long-axis of the whole sequence into account, Node 2 in focal mechanism is speculated to be fault plane, showing a left-lateral strike-slip faulting, which is consistent with the movement of the Xianshuihe fault zone and the local stress map. From the geometry distribution status and the relationship between the sequence and the faults nearby, it can be inferred that the Moxi fault segment of the Xianshuihe fault zone is the seismogenic tectonics of the M_S6.8 Luding earthquake.

Contributions: M.Z. and F.L. mainly completed the data processing and writing of the manuscript. F.D. supported the completion of the manuscript. Y.G. participated worked for the manuscript. All authors contributed to the article and approved the submitted version.

Acknowledgments: The b-value calculation in this article comes from the ZMAP package (Wiemer, 2001); a part of the figures in the paper were plotted with GMT (Wessel and Smith, 1991). We also would like to thank the reviewers for their helpful comments.

Funding: This research was funded by State Key Laboratory of Geodesy and Earth's Dynamics, Innovation Academy for Precision Measurement Science and Technology, CAS, grant number SKLGED2023-4-5.

Conflicts of Interest: The authors declare no conflict of interest. The funders had no role in the design of the study; in the collection, analyses, or interpretation of data; in the writing of the manuscript, or in the decision to publish the results.

References

[1] Molnar P, Qidong D. Faulting associated with large earthquakes and the average rate of deformation in Central and eastern Asia[J]. *Journal of Geophysical Research Atmospheres*, **1984**,89(B7):6203-6228. DOI: https://doi.org/10.1029/JB089iB07p06203.

[2] Tang R C, Han W B. *Active faults and earthquakes in Sichuan*[M]. Seismological Press: Beijing, China, **1993**.

[3] Wang Z X, Xu Z Q, Yang T N, Hao M Y. Study of Deformation mechanism of The Xianshuihe River Fault Zone-A Shallow-Level, High-temperature Ductile Shear Zone[J]. *Regional Geology of China*, **1996**,(3):244-251. DOI: https://doi.org/10.1007/BF02951625.

[4] Xu Z Q, Hou L W, Wang Z X. *Orogenic Process of the Songpan-Ganzi Orogenic Belt in China*[M]. Geological Publishing House: Beijing, China, **1992**.

[5] Qian H, Luo Z L, Wen X Z. Preliminary study of characteristic earthquakes in the Xianshuihe Fault Zone[J]. *Acta Seismological Sinica*, **1990**,12(1):22-29+115. DOI: https://doi.org/CNKI:SUN:DZXB.0.1990-01-003.

[6] Wen X Z, Allen C A, Luo Z L, Qian H, Zhou H W, Huang W S. Segmentation, geometric features and seismotectonic implications of the Holocene Xianshuihe fault Zone[J]. *Acta Seismologica Sinica*, **1989**,11(4):362-372. DOI: https://doi.org/CNKI:SUN:DZXB.0.1989-04-002.

[7] Allen C R, Luo Z L, Qian H, Wen X Z, Zhou H W, Huang W S. Field study of a highly active fault zone: The Xianshuihe fault of southwestern China[J]. *Geological Society of America Bulletin*, **1991**,103(9):1178-1199. DOI: https://doi.org/10.1130/0016-7606(1991)1032.3.CO;2.

[8] Zhou R J, He Y L, Huang Z Z, Li X G, Yang T. The slip rate and strong earthquake recurrence interval on the Qianning-Kangding segment of the Xianshuihe fault zone[J]. *Acta Seismological Sinica*, **2001**,14(3):263-273. DOI: https://doi.org/10.1007/s11589-001-0004-8.

[9] Shi L B, Lin C Y, He Y N, Liu X S, Chen X D. Fault Rocks and Activities of the Kangding-Moxi Fault Zone[J]. *Seismology And Geology*, **1992**,14(2):97-104+193-194. DOI: https://doi.org/10.1159/000227033.

[10] Wen X Z. Character of rupture segmentation of the Xianshuihe-Anninghe-Zemuhe Fault Zone, Western Sichuan[J]. *Seismology And Geology*, **2000**,3(3):60-64. DOI: https://doi.org/10.1088/0305-4470/7/3/008.

[11] Wen X Z, Fan J, Yi G X, Deng Y W, Long F. A seismic gap on the Anninghe fault in western Sichuan, China[J]. *Science in China Series D: Earth Sciences*, **2008**,51(10):1375-1387. DOI: https://doi.org/10.1007/s11430-008-0114-4.

[12] Wiemer S. Minimum Magnitude of Completeness in Earthquake Catalogs: Examples from Alaska, the Western United States, and Japan[J]. *Bull.seismol.soc.am*, **2000**,90(4):859-869. DOI: https://doi.org/10.1785/0119990114.

[13] Gutenberg B, Richter C F. Frequency of Earthquakes in California[J]. *Bulletin of the Seismological Society of America*, **1994**,34(4):185-188.

[14] Omori, F. On the aftershocks of earthquakes[J]. *Journal of the College of Science, Imperial University of Tokyo*, **1894**,7:111–200.

[15] Utsu T, Ogata Y, Ritsuko S, Matsu'ura. The Centenary of the Omori Formula for a Decay Law of Aftershock Activity[J]. *Journal of Physics of the Earth*, **1995**,43(1):1-33. DOI: https://doi.org/10.4294/jpe1952.43.1.

[16] Jiang H K, Dai L, Hou H F, Hua A J, Zheng J C. Statistic study on the criterion index for classification of aftershock sequences[J]. *Earthquake*, **2006**,26(3):17-25. DOI: https://doi.org/10.1007/s11442-006-0415-5.

[17] Zhou H L, Fang G R, Zhang A D, Li Y F, Ke L S, Du Y H. Discussion on the method of judging earthquake type[J]. *Northwestern Seismological Journal*, **1980**,2(2):45-59.

[18] Gutenberg R C, Richter F. Magnitude and Energy of Earthquakes[J]. *Nature*, **1955**,176(4486):795-795. DOI: https://doi.org/10.1038/176795a0.

[19] Qi Y P, Long F, Lin S J, Xiao B F, Zhao X Y, Wang P L, Feng J G. A study on the earthquake sequence type in the middle section of the north-south seismic belt and its surrounding regions[J]. *Seismology and Geology*, **2021**,43(1):177-196. DOI: https://doi.org/10.3969/j.issn.0253-4967.2021.01.011.

[20] Zhang Z C. *Chinese earthquake cases (1966-1975)*[M]. Seismological Press: Beijing, China, **1988**.

[21] Zhang Z C. *Chinese earthquake cases (1981-1985)*[M]. Seismological Press: Beijing, China, **1990**.

[22] Hardebeck J L, Shearer P M. A New Method for Determining First-Motion Focal Mechanisms[J]. *Bull.seism.soc.am*, **2002**,92(6):2264-2276. DOI: https://doi.org/10.1785/0120010200.

[23] Hardebeck J L, Shearer P M. Using S/P Amplitude Ratios to Constrain the Focal Mechanisms of Small Earthquakes[J]. *Bulletin of the Seismological Society of America*, **2003**,93(6):2434-2444. DOI: https://doi.org/10.1785/0120020236.

[24] Yang Z G, Dai D Q, Zhang Y, Zhang X M, Liu J. Rupture process and aftershock mechanisms of the 2022 Luding *M*6.8 earthquake in Sichuan, China[J]. *Earthquake Science*, **2022**,35(6):474-484. DOI: https://doi.org/10.1016/j.eqs.2022.09.001.

[25] Hu Y S, Li Z Y, Liu R F, Wang Z B. Focal mechanism of Luding *M*6.8 earthquake, September 2022, and analysis of the loading role of the tectonic stress on the seismogenic fault[J]. *Earthquake Research Advances*, **2023**,3(3):100216. DOI: https://doi.org/10.1016/j.eqrea.2023.100216.

[26] Li G H, Wang A J, Gao Y. Source rupture characteristics of the September 5, 2022, Luding *M*s6.8 earthquake at the Xianshuihe fault zone in southwest China[J]. *Earthquake Research Advances*, **2023**,3(2):100201. DOI: https://doi.org/10.1016/j.eqrea.2022.100201.

[27] An Y R, Wang D, Ma Q, Yueren Xu, Yu Li a, Yingying Zhang, Zhumei Liu, Chunmei Huang, Jinrong Su, Jilong Li, Mingxiao Li, Wenkai Chen, Zhifan Wan, Dengjie Kang, Baoshan Wang. Preliminary report of the September 5, 2022, *M*s 6.8 Luding earthquake, Sichuan, China[J]. *Earthquake Research Advances*, **2023**,3(1): 100184. DOI: https://doi.org/10.1016/j.eqrea.2022.10018.

[28] Cheng E L. Recent tectonic stress field and tectonic movement of the Sichuan Province and its vicinity[J]. *Acta Seismologica Sinica*. **1981**,3(3):231-241. DOI: https://doi.org/ CNKI:SUN:DZXB.0.1981-03-001.

[29] Xie F R, Zhu J Z, Liang H Q, Liu G X. Basic characteristics of recent tectonic stress field in southwest China[J]. *Acta Seismologica Sinica*, **1993**,6(4):843-855. DOI: https://doi.org/10.1007/BF02651820.

[30] Yang S X, Yao R, Cui X F, Chen Q C. Analysis of the characteristics of measured stress in Chinese mainland and its active blocks and North-South seismic belt[J]. *Chinese Journal of Geophysics*, **2012**,55(12):4207-4217. DOI: https://doi.org/10.6038/j.issn.0001-5733.2012.12.032.

[31] Guo R, Zheng Y, Xu J Q. Stress modulation of the seismic gap between the 2008 *M*s8.0 Wenchuan earthquake and the 2013 *M*s7.0 Lushan earthquake and implications for seismic hazard[J]. *Geophysical Journal International*, **2020**,221(3):2113-2125. DOI: https://doi.org/10.1093/gji/ggaa143.

[32] Yang W, Cheng J, Liu J, Zhang X. The Kangding earthquake swarm of November 2014[J]. *Earthquake Science*, **2015**,28(3):197-207. DOI: https://doi.org/10.1007/s11589-015-0123-2.

[33] Wang J, Xu C, Freymueller J T, Li, Z. Probing Coulomb stress triggering effects for a *M*w > 6.0 earthquake sequence from 1997 to 2014 along the periphery of the Bayan Har block on the Tibetan Plateau[J]. *Tectonophysics*, **2016**,694:249-267. DOI: https://doi.org/10.1016/j.tecto.2016.11.009.

(Executive Editor: Jia-qi Wu)